Structure-Guided Design of C_2-Symmetric HIV-1 Protease Inhibitors Based on a Pyrrolidine Scaffold†

Andreas Blum,‡ Jark Böttcher,‡ Andreas Heine, Gerhard Klebe, and Wibke E. Diederich*

Institut für Pharmazeutische Chemie, Philipps-Universität Marburg, Marbacher Weg 6, 35032 Marburg, Germany

Received September 13, 2007

Infections with the human immunodeficiency virus, which inevitably lead to the development of AIDS, are still among the most serious global health problems causing more than 2.5 million deaths per year. In the pathophysiological processes of this pandemic, HIV protease has proven to be an invaluable drug target because of its essential role in the virus' replication process. By use of pyrrolidine as core structure, symmetric 3,4-bis-*N*-alkylsulfonamides were designed and synthesized enantioselectively from D-(−)-tartaric acid as a new class of HIV protease inhibitors. Structure-guided design using the cocrystal structure of an initial lead as starting point resulted in a second series of inhibitors with improved affinity. The binding modes of four representatives were determined by X-ray crystallography to elucidate the underlying factors accounting for the SAR. With this information for further rational design, the combination of suitable side chains resulted in a final inhibitor showing a significantly improved affinity of $K_i = 74$ nM.

Introduction

Infection with the human immunodeficiency virus (HIV[a]) inevitably leads to the development of the acquired immune deficiency syndrome (AIDS). The WHO estimates that currently 40 million people are infected worldwide and that this number will increase continuously.[1] In the past 20 years, chemotherapy against HIV infection has been tackled by modern drug discovery and development. Several stages in the viral replication have been targeted to reduce the viral load, thus delaying the progression to AIDS. However, an entire remedy of the infection or a vaccination is still an unaccomplished goal.[2] One of the most successful approaches in antiviral therapy up to date is the highly active antiretroviral therapy (HAART) which combines inhibitors of the viral reverse transcriptase and the viral protease. This viral protease, the HIV protease, belongs to the class of aspartic proteases and cleaves precursor polypeptides into functional viral proteins, which are essential for the infectiousness of the virus particles. The HIV protease is a C_2-symmetric homodimer with each monomer consisting of 99 residues. Two glycine-rich flaps are located above the large active site, which binds six to seven amino acids of the nine different cleavage sites within the gag and pol polypeptides. Because inhibition of this enzyme leads to immature virions, HIV protease has become a target of several marketed drugs. Up to now, nine inhibitors against the HIV protease have been approved by the FDA,[3–6] but meanwhile the virus has shown a very high degree of adaptability. The high mutation rate of the virus is caused by the error-prone viral reverse transcriptase and its fast replication rate. This leads, especially under the additional selection pressure of HAART, to the development of resistant virus variants.[7] Because a similar mode of action of all approved inhibitors has resulted in pronounced cross resistance, the need of a steadfast and continuous search for new inhibitors is evident. An increased structural diversity of inhibitor scaffolds could be a possible strategy to at least diminish the accelerated development of multidrug resistant variants.

Most of the approved inhibitors are transition state mimetics addressing the catalytic dyad (D25A/D25B) via a hydroxyl group. As a different approach, cyclic amines have been identified as nonpeptidic inhibitors for the aspartic proteases renin,[8,9] β-secretase,[10] and plasmepsins.[11,12] Recently, a pyrrolidine-based inhibitor for HIV protease has been developed.[13,14] The X-ray structure of the protein inhibitor complex revealed the endocyclic amino function binding to the catalytic dyad. Electrostatic calculations suggest that the amino functionality should be protonated and both aspartic acid residues of the catalytic dyad therefore deprotonated, thus leading to strong hydrogen bonds as well as electrostatic interactions of the resulting cyclic ammonium function with the catalytic dyad.[15] The sulfonamide side chain of the inhibitor addresses the flap region by one of its oxygen atoms through hydrogen bonding to the backbone NH of I50A (Figure 1). A superposition of this structure with other crystal structures of HIV protease complexes indicated that the distance between the sulfonyl group and the endocyclic nitrogen is too large for appropriate flap interactions. The carboxamide part of inhibitor **1** showed no directed polar interactions to the enzyme and was therefore not considered for further inhibitor design.

Guided by the described polar interactions of inhibitor **1** to the enzyme, a basic pharmacophore model was derived. As core structure, the 3*S*,4*S*-disubstituted pyrrolidine, addressing the catalytic dyad via its secondary amino group, was retained. However, as indicated by the X-ray structure of **1**, the exocyclic methylene groups were removed in order to improve the interaction pattern of the sulfonyl groups with the flap region of the enzyme. To exploit the C_2 symmetry of the enzyme, exclusively symmetric inhibitors were synthesized. To mimic the subpocket occupation of **1**, arylsulfonamides were introduced to occupy the S_2- and S_2'-subpockets. In addition, a hydrophobic

† PDB codes: **6ad**, 2PQZ; **6af**, 2QNP; **6cd**, 2QNQ; **6fd**, 2PWR; **6gd**, 2PWC; **6fg**, 2QNN.

* To whom correspondence should be addressed. Phone: +49-6421-28-25810. Fax: +49-6421-28-26254. E-mail: wibke.diederich@staff.uni-marburg.de.

‡ Equally contributing authors.

[a] Abbreviations: AIDS, acquired immunodeficiency syndrome; FDA, Food and Drug Administration; HAART, highly active antiretroviral therapy; HIV, human immunodeficiency virus; rmsd, root-mean-square deviation; SAR, structure–activity relationship; vdW, van der Waals; WHO, World Health Organization.

10.1021/jm701142s CCC: $40.75
Published on Web 03/19/2008

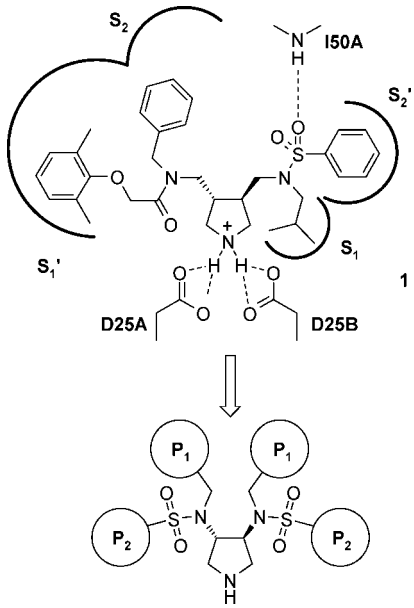

Figure 1. Design of C_2-symmetric inhibitors starting from the cocrystal structure of **1**.

Scheme 1[a]

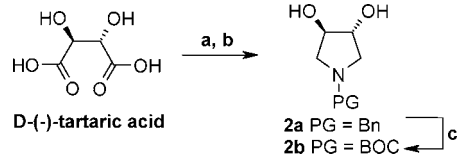

[a] (a) $BnNH_2$, xylene, Dean–Stark (81%); (b) LAH, THF, reflux (69%); (c) H_2, Pd/C, BOC_2O, MeOH (74%).

moiety was attached to each of the sulfonamide nitrogen atoms designed to address the S_1- and S_1'-subsites of the enzyme (Figure 1).

Chemistry

3,4-Difunctionalized pyrrolidines are accessible in enantiopure form commencing with commercially available tartaric acids.[16,17] D-(−)-Tartaric acid was condensed with benzylamine to furnish the corresponding cyclic imide, which was further reduced with $LiAlH_4$ to yield the benzyl-protected pyrrolidine-3,4-diol **2a**[18] (Scheme 1). The synthesis of the corresponding benzyl protected pyrrolidine-3,4-diamine, accessible via a Mitsunobu reaction of diol **2a** with HN_3 and subsequent reduction of the resulting diazide, has already been described.[19] However, following this synthetic route, the removal of the benzyl-protecting group by catalytic hydrogenation in the last step of the synthesis to give rise to the final inhibitors remained unsuccessful, even after applying higher temperature and hydrogen pressure as well as different hydrogen sources. Furthermore, we intended to avoid the usage of the very toxic hydrazoic acid in the Mitsunobu reaction. Therefore, a change to the easily removable BOC protecting group was necessary. This exchange was carried out at the diol stage by hydrogenation of **2a** in the presence of BOC_2O,[20] yielding the BOC-protected 3,4-diol **2b** (Scheme 1). Although an activation of the 3,4-pyrrolidine diol for the purpose of nucleophilic displacement reactions by conversion into its corresponding disulfonates has been described,[21,22] in our hands, the respective mesylate did not undergo substitution with NaN_3 in DMSO even at 120 °C. Nevertheless, utilization of the related but significantly more reactive bis-triflate **2c** followed by its nucleophilic substitution with NaN_3 in DMPU at room temperature now yielded the 3,4-diazide **2d**, which was subsequently reduced to the corresponding pyrrolidine diamine **3** by catalytic hydrogenation (Scheme 2) in excellent overall yield.

Scheme 2[a]

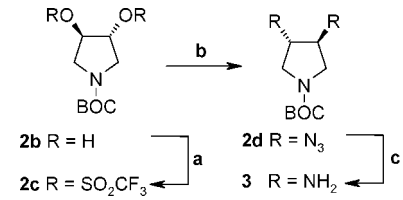

[a] (a) Tf_2O, pyridine, CH_2Cl_2 −78 to −10 °C; (b) NaN_3, DMPU, room temp; (c) H_2, Pd/C, hexane/EtOAc (86% over three steps).

Scheme 3[a]

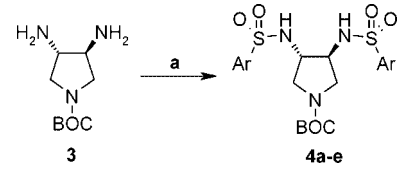

[a] (a) $ArSO_2Cl$, Et_3N, CH_2Cl_2. **4a**: Ar = Ph (86%). **4b**: Ar = *o*-Me-Ph (87%). **4c**: Ar = *o*-Cl-Ph (94%). **4d**: Ar = *p*-NO_2-Ph (69%). **4e**: Ar = *p*-CN-Ph (71%).

Scheme 4[a]

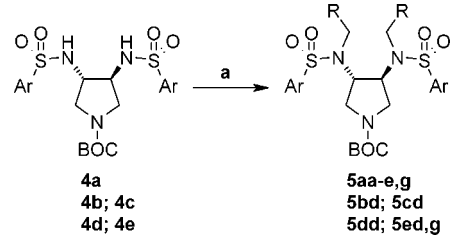

[a] (a) RCH_2Br, K_2CO_3, CH_3CN, reflux. **4a**: Ar = Ph. (**5aa**: R = CH=CH_2, 72%. **5ab**: R = $CH(CH_3)$=CH_2, 73%. **5ac**: R = CH=$C(CH_3)_2$, 68%. **5ad**: R = Ph, 75%. **5ae**: R = *p*-Br-Ph, 76%. **5af**: R = *p*-I-Ph, 76%. **5ag**: R = *p*-CF_3-Ph, 49%.) **4b**: Ar = *o*-Me-Ph. (**5bd**: R = Ph, 78%.) **4c**: Ar = *o*-Cl-Ph. (**5cd**: R = Ph, 65%.) **4d**: Ar = *p*-NO_2-Ph. (**5dd**: R = Ph, 96%.) **4e**: Ar = *p*-CN-Ph. (**5ed**: R = Ph, 67%. **5eg**: R = *p*-CF_3-Ph, 45%.)

Scheme 5[a]

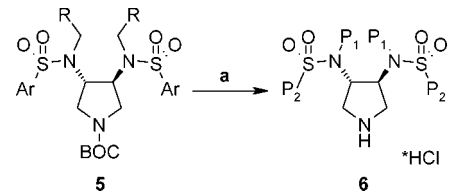

[a] (a) 2 M HCl in Et_2O, room temp. Details are given in Table 1.

Diamine **3** was then condensed with suitable sulfonyl chlorides to the corresponding sulfonamides **4** (Scheme 3), which were further alkylated with different allyl and benzyl bromides in the presence of K_2CO_3 in acetonitrile (Scheme 4), thus yielding the BOC-protected inhibitor precursors of type **5**. The final deprotection was carried out under nonaqueous acidic conditions using 2 M HCl in Et_2O, furnishing the inhibitors **6** as their hydrochlorides in high yields (Scheme 5; yields are given in Table 1). In compounds with double lettering codes, the first letter refers to the sulfonyl substituents (P_2/P_2'), the second letter to the *N*-alkyl moieties (P_1/P_1').

The carboxamido-substituted compounds **5fd**, and **5fg** are accessible from the corresponding cyano-substituted derivatives **5ed** and **5eg** by mild hydrolysis, applying 30% H_2O_2 in DMSO

Table 1. K_i Values of the Inhibitors **6** toward the HIV Protease and Yield of the Terminal Deprotection Step

	P_2/P_2'	P_1/P_1'	K_i [μM]	Yield (from **5**)
6aa			12.3	76 (**5aa**)
6ab			74.7	71 (**5ab**)
6ac			1.57	78 (**5ac**)
6ad		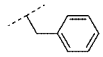	2.15	92 (**5ad**)
6ae		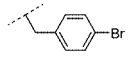	0.46	72 (**5ae**)
6af		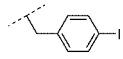	0.39	81 (**5af**)
6ag		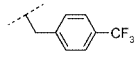	0.80	71 (**5ag**)
6bd		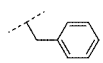	0.67	81 (**5bd**)
6cd		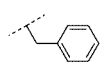	0.77	78 (**5cd**)
6dd	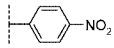	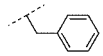	1.72	79 (**5dd**)
6fd	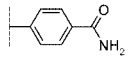	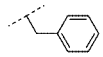	0.26	81 (**5fd**)
6gd	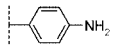	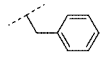	0.27	79 (**5dd**)
6fg	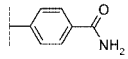	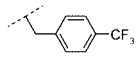	0.07	80 (**5fg**)

(Scheme 6).[23] The amino-substituted inhibitor **6gd** was obtained from the corresponding nitro-substituted precursor **5dd** by reduction with $SnCl_2$ in EtOAc at elevated temperature.[24] Under these reaction conditions, the BOC protecting group was removed simultaneously (Scheme 7). The synthesis of inhibitors of type **6** was achieved in seven or eight steps, respectively, starting from D-(−)-tartaric acid in an overall yield ranging from 7% to 21% with an average yield of more than 70% for each step.

Results and Discussion

To gain the first insight into the structure–activity-relationship (SAR), the benzene sulfonamide group in **4a** was alkylated with three differently alkyl-substituted alkenyl moieties and a benzyl group using allyl bromide (to **5aa**), 2-methylallyl bromide (to **5ab**), 3,3-dimethylallyl bromide (to **5ac**), and benzyl bromide (to **5ad**). After acidic deprotection of the BOC group, inhibitors **6aa**−**ad** were obtained. All four bis-substituted sulfonamides showed affinity in the micromolar range against HIV protease, from which those inhibitors with the largest moieties (**6ac** and **6ad**) exhibited the highest affinity (Table 1).

The X-ray structure of **6ad** in complex with the protease was determined with a resolution of 1.55 Å and surprisingly revealed an asymmetric binding mode (Figure 2). Similar to the complex

Scheme 6[a]

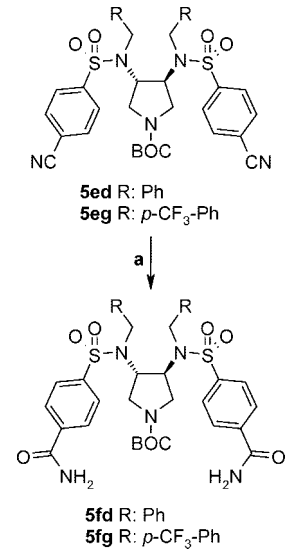

[a] (a) 30% aqueous H_2O_2, K_2CO_3, DMSO, 0 °C to room temp. (**5fd**: R = Ph, 92%. **5fg**: R = *p*-CF_3-Ph, 71%.)

Scheme 7[a]

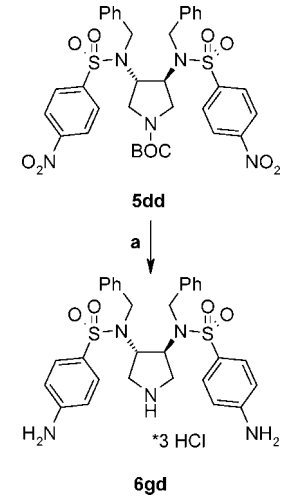

[a] (a) $SnCl_2 \cdot 2\ H_2O$, EtOAc, 2 h reflux, then 2 M HCl in Et_2O 79%.

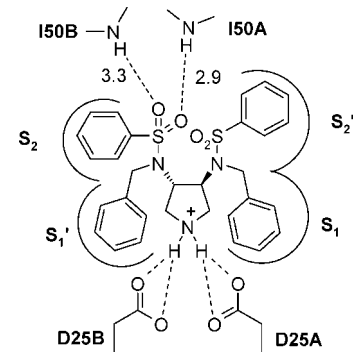

Figure 2. Schematic representation of the binding mode of **6ad** observed in the crystal structure in complex with the HIV protease. Bond lengths to I50A and I50B of the flap region are given in Å.

structure of pyrrolidine-based inhibitor **1**, the protonated cyclic amino nitrogen is found at its pivotal position forming a hydrogen bond network to the catalytic aspartic acid residues D25A (2.6, 3.0 Å) and D25B (2.9, 3.0 Å). Instead of a structural water molecule usually present in peptidomimetic or substrate-

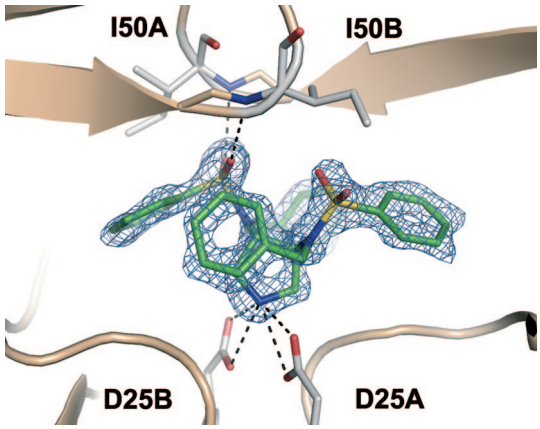

Figure 3. Crystal structure of **6ad** (green, coded by atom type) in complex with HIV protease. The protein backbone trace is schematically illustrated in wheat, the catalytic D25A and D25B as well as I50A and I50B of the flaps are displayed in gray, coded by atom type. The $F_o - F_c$ density for the ligand is displayed at a σ level of 3.0 as blue mesh.

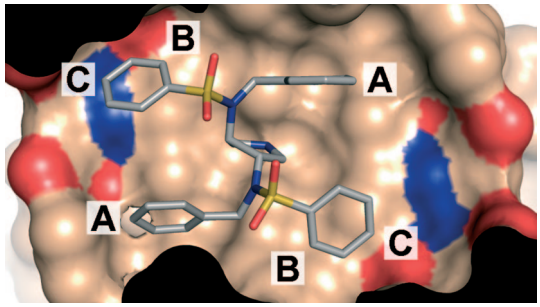

Figure 4. Overview of the optimization strategies of **6ad** by attachment of additional substituents. Protein is shown in wheat surface representation. D29 and D30 surface patches are shown in color, coded by atom type: (A) hydrophobic P_1/P_1' elongation; (B) small hydrophobic P_2/P_2' ortho substitution; (C) polar P_2/P_2' para substitution to address D29 and D30.

like complexes, one sulfonyl group establishes two hydrogen bonds to the backbone NHs of I50A (2.9 Å) and I50B (3.3 Å), each with one sulfonyl oxygen atom. The second sulfonyl group, however, does not form any polar interactions (Figure 3). The benzyl substituents occupy the S_1/S_1'-subpockets, establishing van der Waals (vdW) contacts with L23A, I50B, V82A, I84A (S_1) and R8B, L23B, I50A, P81B, V82B, I84B (S_1'). The phenyl moieties reside in the S_2/S_2'-subsites forming vdW contacts with A28B, V32B, I50A, I84B (S_2) and A28A, D30A, V32A, I47A, I50B (S_2'). Additional vdW contacts are found to G27, G48, and G49 of each subunit. The deviation from a C_2-symmetrical occupation of the subpockets can be analyzed by superpositioning the observed geometry of the inhibitor with its geometry resulting from a rotation around the protein's C_2-axis. The average distance of the corresponding ring atoms is 1.7 Å in the S_1- and 2.1 Å in the S_2-pocket.

This crystal structure enabled us to rationally design the second series of most likely more potent inhibitors. Consequently, **6ad** was selected as lead structure for further optimization. An in-depth analysis of the crystal structure revealed three very promising symmetric substitution patterns for further lead optimization (Figure 4): (A) elongation of the P_1/P_1'-benzyl moieties with hydrophobic substituents in para position to address unoccupied space in the S_1/S_1'-pocket; (B) ortho substitution at the P_2/P_2'-phenyl ring systems to improve the shape match between the binding pocket surface and the ligand,

Table 2. Conserved Hydrogen Bonds of the Pyrrolidine Nitrogen Atom to the Catalytic Dyad (D25A/D25B) and the Sulfonyl Oxygen Atoms to the Flap (I50A/I50B) Observed in the Determined Cocrystal Structures[a]

	6ad	**6af**	**6cd**	**6fd**	**6gd**	**6fg**
D25A $O_{\delta 1}$	3.0	2.9	3.0	3.0	3.0	2.9
D25A $O_{\delta 2}$	2.6	2.7	2.5	2.7	2.6	2.7
D25B $O_{\delta 1}$	3.0	2.8	2.8	2.8	2.8	2.8
D25B $O_{\delta 2}$	2.9	3.1	2.9	2.8	2.9	3.0
I50A N	2.9	3.0	3.1	3.0	3.1	2.9
I50B N	3.3	3.1	3.6	3.2	3.7	3.1

[a] Values are given in Å.

where for this purpose small hydrophobic substituents were selected in order to fill remaining space flanked by V32B and I84B in the S_2-pocket as well as V32A and I84A in the S_2'-pocket; (C) para substitution at the P_2/P_2'-phenyl moieties with substituents capable of forming hydrogen bonds to D29A and D30A in the S_2'-pocket and D29B and D30B in the S_2-pocket.

All three strategies were pursued, and the resulting inhibitors **6ae**−**ag** and **6bd**−**gd** were subsequently analyzed by kinetic measurements with respect to their affinity against the target enzyme. The cocrystal structures of selected representatives, at least one of each modification type, in complex with HIV protease were determined. This approach allows the detailed analysis of additional interactions formed by the introduced substituents and provides an extensive understanding of the principles accounting for the SAR. Subsequently, this knowledge should facilitate the selection of the most promising combination of substituents, thus leading to an even further improved inhibitor.

(A) Elongation of the P_1-benzyl ring in the para position with hydrophobic residues was easily achieved by alkylation of benzene sulfonamide **4a** with appropriately substituted benzyl bromides, yielding after deprotection the corresponding bromo- (**6ae**), iodo- (**6af**), and trifluoromethyl- (**6ag**) substituted inhibitors. These inhibitors indeed showed improved affinity by a factor of 5 compared to **6ad** for the halide substituted ones (**6ae**, 0.46 μM; **6af**, 0.39 μM). In the case of the trifluoromethyl-substituted inhibitor **6ag**, a factor of 3 (0.80 μM) is achieved. The crystal structure of **6af** in complex with HIV protease was determined with a resolution of 1.41 Å and revealed a binding mode resembling that of the unsubstituted pyrrolidine **6ad**. A similar hydrogen-bond network of the core structure can be observed (Table 2). The root-mean-square deviation (rmsd) between the C_α atoms of the complexes of **6ad** and **6af** is 0.15 Å, resembling the overall similar binding mode. This similarity is also reflected by an rmsd of 0.45 Å from the respective **6ad** substructure in **6af**. The gain in affinity is presumably due to additional vdW interactions in the S_1-subsite with P81A, G48B, and G49B and in the S_1'-subsite with R8B. Obviously, the position and orientation of the P_2/P_2'-moiety are not affected by the additional substituent.

(B) The extension of the P_2/P_2'-phenyl ring in the ortho position with small hydrophobic substituents was successfully accomplished by synthesis of the *o*-methyl and *o*-chloro substituted benzene sulfonamides **4b** and **4c**, respectively, which were subsequently alkylated with benzyl bromide yielding after deprotection the methyl- (**6bd**) and chloro- (**6cd**) substituted inhibitors. Compared to the lead structure **6ad**, a 3-fold increase in affinity was observed (**6bd**, 0.67 μM; **6cd**, 0.77 μM). The 2.30 Å resolved crystal structure of the chloro derivative **6cd** revealed a similar binding mode compared to that of **6ad**. The protein structure remains unaffected (C_α rmsd to **6ad** is 0.14 Å); however, the binding mode of **6cd** slightly deviates from the expected conformation (rmsd to **6ad** substructure is 0.67

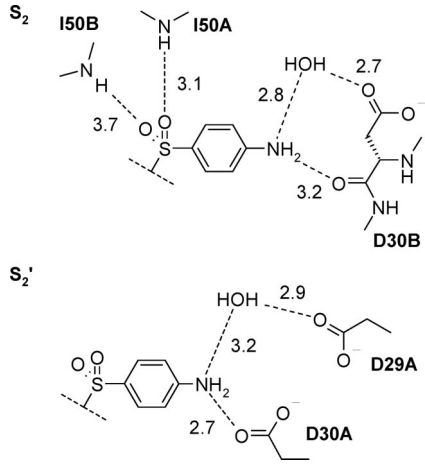

Figure 5. Schematic representation of the hydrogen bond network observed in the crystal structure of **6gd**. Bond lengths are given in Å.

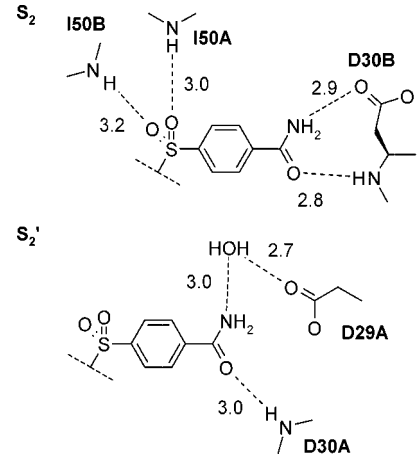

Figure 6. Schematic representation of the hydrogen bond network observed in the crystal structure of **6fd**. Bond lengths are given in Å.

Å). The observed polar interactions are in agreement with the structure of **6ad** (Table 2); furthermore, the *o*-chloro substitution is as intended in additional vdW contacts of the chlorine atom to V32B and I84B in the S_2'-pocket. Moreover, the ortho substituent induces an unanticipated change in the orientation of the phenyl moiety in the S_2-pocket. There, the chloro substituent points in the opposite direction toward the S_1-pocket now interacting with G48B and G49B, hence retaining the orientation of **6ad**.

(C) For the decoration of the P_2/P_2'-phenyl moieties in the para position with polar groups, the 4-nitrophenylsulfonamide **4d** and the 4-cyanophenylsulfonamide **4e** were synthesized and subsequently alkylated with benzyl bromide. The alkylated nitro compound **5dd** was on the one hand directly deprotected to yield inhibitor **6dd**. On the other hand, the nitro group in **5dd** was first reduced to the corresponding amino function, concurrently removing the protecting group now giving rise to the amino-substituted inhibitor **6gd**. The alkylated cyano compound **5ed** was converted into the carboxamide **5fd** and subsequently deprotected yielding inhibitor **6fd**. Compared with the unsubstituted pyrrolidine **6ad**, the nitro-substituted inhibitor **6dd** only showed a comparable affinity (**6dd**, 1.72 μM), whereas those inhibitors with hydrogen bond donor substituents revealed an 8-fold increase in affinity (**6fd**, 0.26 μM; **6gd**, 0.27 μM). To elucidate the hydrogen bond network established by the polar substituents, both inhibitors were crystallized in complex with HIV protease and the resulting crystal structures were determined (resolution: **6fd**, 1.50 Å; **6gd**, 1.78 Å). Both crystal structures show a high similarity to that of **6ad** with respect to the C_α atoms of the protein (C_α rmsd **6fd**, 0.25 Å; **6gd**, 0.12 Å) as well as the binding mode of the ligand (rmsd of **6ad** substructure **6fd**, 0.54 Å; **6gd**, 0.36 Å). The polar interactions of the central scaffold are similar to those of **6ad** (Table 2). Because of the asymmetric binding mode, the interaction patterns in the S_2- and S_2'-subpockets of each ligand differ from each other (Figures 5 and 6). The *p*-amino derivative **6gd** establishes two hydrogen bonds in the S_2-pocket, one directly to the backbone carbonyl of D30B (3.2 Å) and one to the side chain of D30B bridged by a water molecule (2.8, 2.7 Å). In the S_2'-pocket, two hydrogen bonds are also formed, however, now to the side chains of D30A (2.7 Å) and D29A again mediated by an interstitial water molecule (3.2, 2.9 Å). The same number of hydrogen bonds can be observed for the *p*-carboxamido substituted inhibitor **6fd**. In the S_2-pocket the backbone NH of D30B is addressed via the carboxamide oxygen (2.8 Å), whereas the amide nitrogen establishes a hydrogen bond to the side chain of D30B (2.9 Å). In the S_2'-pocket a water molecule mediates the interaction between the ligand amido nitrogen and the D29A side chain (3.0, 2.7 Å). The carbonyl function of the ligand accepts a hydrogen bond from the backbone NH of D30A (3.0 Å). The position of the P_1/P_1'-residues in both ligand structures is not affected by these additional interactions in the S_2- and S_2'-pockets.

Table 3. Calculated rmsd after Alignment of the Protein C_α Atoms[a]

	6ad	6af	6cd	6fd	6gd	6fg
			Protein C_α			
6ad		0.15	0.14	0.25	0.12	0.19
6af	0.15		0.17	0.23	0.19	0.18
6cd	0.14	0.17		0.28	0.15	0.20
6fd	0.25	0.23	0.28		0.23	0.23
6gd	0.12	0.19	0.15	0.23		0.20
6fg	0.19	0.18	0.20	0.23	0.20	
			6ad Substructure			
6ad		0.45	0.67	0.54	0.36	0.69
6af	0.45		0.56	0.66	0.57	0.61
6cd	0.67	0.56		0.85	0.72	0.81
6fd	0.54	0.66	0.85		0.28	0.32
6gd	0.36	0.57	0.72	0.28		0.48
6fg	0.69	0.61	0.81	0.32	0.48	

[a] For the ligands the respective **6ad** substructure within each ligand is compared after C_α-alignment of the protein structure. Values are given in Å.

All crystal structures analyzed at this stage of the project are very similar; the rmsd between the C_α atoms of any two complexes is less than 0.28 Å, and all inhibitors also show a very high degree of similarity in their binding modes (Table 3). The hydrogen-bond network of the lead structure **6ad** is conserved in all structures (Table 2). The rmsd between the respective substructure and **6ad** is less than 0.69 Å. For the comparison of any two ligands, the rmsd is less than 0.85 Å. The largest differences are observed between the *o*-chloro-substituted ligand (**6cd**) and the *p*-amino (**6gd**) or the *p*-carboxamido-substituted ligand (**6fd**) with 0.72 and 0.85 Å, respectively. This reflects the different binding mode of **6cd** (Table 3). This different binding mode makes an ortho substitution at the P_2-residue less attractive for further combination with other modifications (Figure 7), so only the two remaining substitution strategies were combined. As substituents for the combined inhibitor, a trifluoromethyl group such as P_1/P_1' and a carboxamido moiety such as the P_2/P_2' substituent were selected.

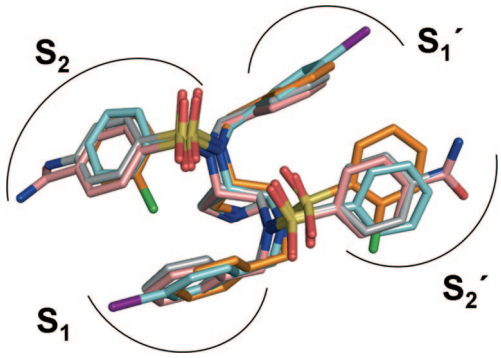

Figure 7. Superposition of the ligand conformations observed in the corresponding crystal structures aligned by C_α-fit of the proteins. Ligands are color-coded by atom type: **6af** (cyan), **6cd** (orange), **6fd** (salmon), **6gd** (gray).

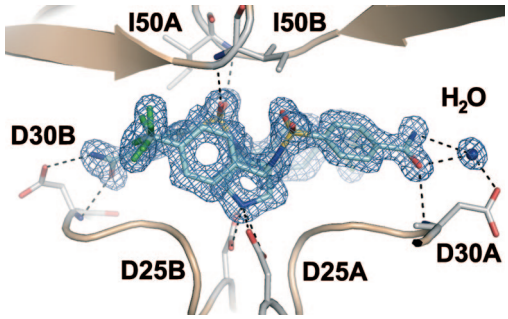

Figure 8. Crystal structure of **6fg** (cyan, coded by atom type) in complex with HIV protease. The protein backbone trace is schematically illustrated in wheat. The catalytic D25A/D25B, D30A/D30B, and I50A/I50B of the flaps are displayed in gray, coded by atom type. The $F_o - F_c$ density for the ligand is displayed at a σ level of 3.0 as blue mesh.

The combined inhibitor **6fg** was prepared in similar manner as already described for carboxamide inhibitor **6fd** starting from sulfonamide **4e**, followed by alkylation to **5eg** and subsequent hydrolysis of the nitriles to the carboxamide **5fg**. After acidic, nonaqueous deprotection, the inhibitor **6fg** was tested for its affinity against HIV protease. With 74 nM, the trifluoromethyl and carboxamido-substituted inhibitor **6fg** exhibits the highest affinity within this series. To validate our combination strategy pursued within this project, the crystal structure of **6fg** in complex with HIV protease was determined with a resolution of 1.48 Å (Figure 8). No major differences could be observed comparing the protein structure to the formerly determined complexes (C_α rmsd to **6af**, 0.18 Å; to **6fd**, 0.23 Å). Our successful combination strategy is also represented in the conserved ligand conformation (rmsd of **6ad** substructure to **6af**, 0.61 Å; **6fd**, 0.32 Å). The polar interaction pattern of the carboxamido-substituted inhibitor **6fd** is retained. Compared to **6af**, additional vdW contacts of the trifluoromethyl group to R8A in the S_1-subsite are observed. In the structure of **6fg**, both CF_3 groups show disorder of a rigid rotor. They were refined as double conformations.

Summary and Conclusion

C_2-symmetric 3,4-disubstituted pyrrolidines have been developed as a new class of HIV protease inhibitors. Starting from the initial lead **6ad**, which showed affinity in the low micromolar range, the activity of this new class of HIV protease inhibitors could be significantly optimized by means of rational structure-based design up to the two digit nanomolar range for the final inhibitor **6fg**. On the basis of our developed synthetic strategy, the synthesis of the enantiopure key intermediate **3** commencing with D-(−)-tartaric acid is straightforward and high-yielding. Condensation of **3** with appropriately chosen sulfonyl chlorides renders the corresponding sulfonamides, alkylation of which, followed by further functional group transformations and deprotection, gave rise to the desired inhibitors. These are obtained via a seven- or eight-step synthesis with an overall yield ranging from 7% to 21%. Following the outlined synthetic route, the synthesis of a plethora of putative protease inhibitors is readily feasible. Initial SAR studies as well as the crystal structure determination resulted in selection of **6ad** as the lead compound for further structural optimization. The analysis of the cocrystal structure of **6ad** revealed three possible strategies for optimization via symmetric introduction of substituents to the original P_1/P_1'- and P_2/P_2'-phenyl moieties. From each class of possible modifications, at least one representative was synthesized and thoroughly analyzed by crystal structure determination of the protein–ligand complex. The observed interactions of the core structure are highly conserved throughout this series of inhibitors. These structures provided deeper insights into the protein–ligand interactions and the underlying principles of the SAR. Taking this information into account, the most promising combination of P_1/P_1'- and P_2/P_2'-moieties was selected and the resulting inhibitor **6fg** indeed showed the expected improvement in affinity with K_i = 74 nM. The cocrystal structure of this inhibitor confirmed the successful application of our optimization strategy. The complete structural characterization of crucial intermediates prevents misdirection by only taking the affinity of the compounds into account. This project clearly shows that the rational design of inhibitors based on the successful cooperation between synthetic medicinal chemistry and structural biology can lead to a highly efficient optimization of lead structures.

Experimental Section

Kinetic Assay. Inhibition data for HIV protease were determined as follows: IC_{50} values were taken from plots of v_i/v_0 versus inhibitor concentration, in which v_i is the velocity in the presence of an inhitor and v_0 is the velocity in the absence of an inhibitor. The fluorogenic substrate Abz-Thr-Ile-Nle-(*p*-NO_2-Phe)-Gln-Arg-NH_2 was purchased from Bachem. Recombinant HIV protease was expressed from *Escherichia coli* and purified as previously described.[25] Enzymatic assays were performed in 172 μL of assay buffer (100 mM MES, 300 mM KCl, 5 mM EDTA, 1 mg/mL BSA, pH 5.5) by the addition of substrate dissolved in 4 μL of DMSO, distinct inhibitor concentrations dissolved in 4 μL of DMSO, and 20 μL of HIV-1 protease in assay buffer to a final volume of 200 μL (final DMSO concentration of 4%). The hydrolysis of the substrate was recorded as the increase in fluorescence intensity (excitation wavelength 337 nm, emission wavelength 410 nm) over 10 min, during which the signal increased linearly with time.[26] The kinetic constants for HIV protease (K_m = 14.6 μM) were determined by the method of Lineweaver and Burk with a HIV protease concentration of 2.8 nM with varied substrate concentrations. The active-site concentration was quantified by titrating three different HIV protease concentrations with the strong binding inhibitor saquinavir (K_i = 0.3 nM). K_i values were calculated from the following equation: $K_i = [IC_{50} - (E_t/2)][1 + (S/K_m)]^{-1}$

Crystallization of HIV Protease Inhibitor Complexes. HIV protease inhibitor complexes were crystallized at 18 °C in 0.1 M BisTris, pH 6.5, 2.0–3.5 M NaCl, and a protein concentration of 7 mg/mL in the space group $P2_12_12$ (crystal data, Table 4). The crystals were obtained by cocrystallization of the enzyme with inhibitor concentrations ranging from 20- to 100-fold the K_i value. Crystals were further optimized using streak-seeding techniques.

Table 4. Crystallographic Data

	6ad, 2PQZ	**6af**,[b] 2QNP	**6cd**, 2QNQ	**6fd**, 2PWR	**6gd**, 2PWC	**6fg**, 2QNN
resolution (Å)	25–1.55	25–1.41	30–2.30	25–1.50	25–1.78	25–1.48
space group	$P2_12_12$	$P2_12_12$	$P2_12_12$	$P2_12_12$	$P2_12_12$	$P2_12_12$
cell dimensions (Å)	$a = 57.5$	$a = 57.4$	$a = 57.6$	$a = 56.8$	$a = 57.3$	$a = 57.4$
	$b = 86.0$	$b = 85.9$	$b = 85.9$	$b = 84.8$	$b = 85.8$	$b = 86.2$
	$c = 46.7$	$c = 46.7$	$c = 46.5$	$c = 46.1$	$c = 46.5$	$c = 46.3$
highest resoln shell (Å)	1.58–1.55	1.43–1.41	2.35–2.30	1.53–1.50	1.81–1.78	1.51–1.48
completeness (%)[a]	96.3 [87.3]	99.5 [94.1]	97.1 [93.9]	92.1 [93.7]	98.2 [99.5]	99.5 [96.4]
I/σ[a]	13.4 [3.0]	21.9 [2.83]	16.1 [5.27]	34.2 [6.6]	13.5 [2.9]	23.5 [3.71]
R_{sym} (%)[a]	8.6 [33.5]	5.0 [33.4]	11.0 [25.2]	3.9 [23.0]	9.7 [46.3]	4.8 [28.7]
resoln in refinement (Å)	10–1.55	10–1.41	25–2.30	10–1.50	10–1.78	10–1.48
R_{cryst} (%), $F > 4\sigma F_o$;F_o	16.4; 18.9	17.6; 19.1	n.d.; 20.5	16.8; 17.8	16.3; 18.9	17.0; 18.4
R_{free} (%), $F > 4\sigma F_o$;F_o	20.4; 23.4	21.3; 22.9	n.d.; 23.9	20.2; 21.6	21.1; 24.5	19.3; 20.9

[a] Values in brackets refer to the highest resolution shell. [b] In the case of **6af**, the ligand occupancy was refined to 63% with respect to the protein. For additional details, refer to Supporting Information.

For cryoprotection the crystals were briefly soaked in mother liquor containing 25% glycerol.

Data Collection, Phasing, and Refinement. The data sets were collected at the synchrotron BESSY II in Berlin/Germany on PSF beamline 14.2 (PDB codes 2PQZ for **6ad**, 2QNP for **6af**, 2PWC for **6gd**, 2QNN for **6fg**), on the EMBL/DESY in Hamburg/Germany on beamline X13 (PDB code 2PWR for **6fd**), both equipped with a MAR-CCD detector, and on a Rigaku R-AXIS IV image plate detector using Cu Kα radiation from an in-house Rigaku rotating anode (PDB code 2QNQ for **6cd**). Data were processed and scaled with Denzo and Scalepack as implemented in HKL2000.[27] The structures were determined by the molecular replacement method with Phaser;[28] one monomer of the 1.5 Å structure of the HIV-1 protease in complex with a pyrrolidine based inhibitor (PDB code 1XL2), and consecutively a monomer of the determined structure (PDB code 2PQZ for **6ad**), was used as the search model. The structure (PDB code 2QNP for **6af**) was determined by single isomorphous replacement with anomalous scattering method (SIR-AS) using the program implemented in the HKL2MAP graphics user interface;[29] the data set of the unsubstituted pyrrolidine was used as native data. The positions of the iodine atoms were identified using SHELXD,[30] and the phase problem was solved with SHELXE.[31] The resulting phases were applied, and after density modification with DM,[32] ARPwARP[33] as implemented in CCP4[34] was used for automated model building.

Refinement was continued with CNS[35] and SHELXL-97.[36] For each refinement step at least 10 cycles of conjugate minimization were performed, with restraints on bond distances, angles, and *B*-values. Intermittent cycles of model building were done with the program COOT.[37] The coordinates have been deposited in the PDB (http://www.rcsb.org/pdb/) with the following access codes: **6ad**, 2PQZ; **6af**, 2QNP; **6cd**, 2QNQ; **6fd**, 2PWR; **6gd**, 2PWC; **6fg**, 2QNN.

General Synthetic Chemistry. Reported yields refer to the analytical pure product obtained by column chromatography or recrystallization. All proton and carbon nuclear magnetic resonance spectra were recorded on a Jeol Eclipse+ spectrometer (^{1}H NMR, 500 MHz; ^{13}C NMR, 125 MHz) using TMS as internal standard (0.0 ppm). ^{13}C spectra were referenced to $CDCl_3$ (77.16 ppm), DMSO-d_6 (39.52 ppm), or MeOH-d_4 (49.00 ppm). The values of chemical shifts (δ) are given in ppm, and coupling constants (J) are given in Hz. Abbreviations are as follows: br = broad, s = singulet, d = doublet, t = triplet, q = quartet, sm = symmetric multiplet, m =multiplet. Mass spectra were obtained from a double focusing sectorfield Micromass VG-Autospec spectrometer. Combustion analyses were determined on a Vario Micro Cube by Elementar Analysen GmbH, and the results indicated by symbols for the elements were within ±0.4% of theoretical values. Melting points were determined using a Leitz HM-Lux apparatus and are uncorrected. Flash chromatography was performed using silica gel 60 (0.04–0.063 mm) purchased from Macherey-Nagel, and solvents are indicated. TLC was carried out using 0.2 mm aluminum plates coated with silica gel 60 F_{254} by Merck and visualized by UV detection. Solvents and reagents that are commercially available were used without further purification unless otherwise noted. Tetrahydrofuran was dried over lithium aluminum hydride and freshly distilled prior to use; other anhydrous solvents were purchased in Sure/Seal bottles from Sigma-Aldrich or Fluka. All moisture sensitive reactions were carried out using oven-dried glassware under a positive stream of argon. Compound **2a** has been prepared according to a literature procedure.[18]

General Procedure A: Arylsulfonamides. An amount of 1.0 mmol of diamine **3** was dissolved in 6 mL of CH_2Cl_2, and 2.4 mmol of triethylamine or diisopropylethylamine and 2.2 mmol of arylsulfonyl chloride were slowly added. The reaction mixture was stirred for 14–20 h and poured into an aqueous saturated NH_4Cl solution (10 mL). The aqueous phase was separated and extracted with MTBE (3 × 10 mL). The combined organic phases were washed with brine (3 × 10 mL), dried over Na_2SO_4, filtered, and evaporated. The residual oil was dissolved in 5 mL of CH_2Cl_2 and added dropwise to 50 mL of vigorously stirred cold hexane. The precipitate was filtered off, washed with hexane, and dried. The resulting product was used in the following steps without further purification.

General Procedure B: Alkylation of Arylsulfonamides. An amount of 1.00 mmol of sulfonamide **4** and 3.00 mmol of anhydrous K_2CO_3 were suspended in 7.5 mL of dry CH_3CN. An amount of 2.40 mmol of benzyl bromide was added, and the mixture was stirred at the given temperature for 4–12 h. After cooling to room temperature, the insoluble material was filtered off and washed with MTBE. The filtrate was evaporated, and the residual oil was purified by flash chromatography.

General Procedure C: Conversion of Nitriles to Amides. An amount of 0.30 mmol of nitrile **5ed** or **5eg** was dissolved in 3 mL of DMSO and cooled to 0 °C. Then 1.5 mL of 30% H_2O_2 and 200 mg (0.15 mmol) of K_2CO_3 were added to the frozen mixture, which was then allowed to warm to room temperature and stirred for an additional 30 min. The solution was cooled to 0 °C, and an amount of 50 mL of H_2O was added. The precipitated product was filtered off and washed with H_2O and dissolved in 5 mL of $CHCl_3$. The solution was washed with H_2O (3 × 10 mL) and brine (10 mL), dried over $MgSO_4$, filtered, and evaporated.

General Procedure D: BOC Deprotection. An amount of 0.20 mmol of BOC-protected pyrrolidine was dissolved in 5 mL of 2 M HCl in Et_2O. After 14 h the solution was decanted from the precipitated hydrochloride, which was washed thoroughly with dry ether and dried in vacuum.

(3*R*,4*R*)-1-BOC-3,4-dihydroxypyrrolidine (2b). An amount of 6.66 g (34.8 mmol) of *N*-benzylpyrrolidine[18] **2a** was dissolved in 100 mL of MeOH followed by the addition of 8.36 g (38.3 mmol) of BOC_2O and 666 mg of Pd/C. After the reaction mixture was stirred under H_2 atmosphere for 16 h, the catalyst was removed by filtration through a pad of Celite and the filtrate was concentrated. The residual yellow oil was dissolved in 25 mL of hot EtOAc, and the product crystallized upon cooling. The crystals were collected by filtration, washed with cold EtOAc, and dried, yielding 4.50 g of the product **2b**. After concentration of the mother liquor, an additional 0.84 g was obtained resulting in an overall yield of 5.34 g (74%) of **2b**. Beige needles; mp 161 °C; ^{1}H NMR ($CDCl_3$) δ 3.94 (tbr, 2H, $J = 3.3$), 3.67 (dd, 1H, $J = 12.0, 4.9$), 3.63 (dd, 1H, $J =$

11.9, 5.0), 3.42 (dd, 2H, J = 12.1, 2.3), 3.37 (dd, 2H, J = 12.1, 2.3), 1.44 (s, 9H); ^{13}C NMR ($CDCl_3$) δ 153.9, 80.5, 64.2, 63.4, 48.8, 48.5, 28.4; MS (ESI) m/z 204 (25, M + H), 221 (5, M + NH_4), 407 (78, 2M + H), 424 (100, 2M + NH_4); HRMS (ESI) m/z calcd for $C_{18}H_{34}N_2O_8 \cdot NH_4$ 424.265 891, found 424.264 370. Anal. ($C_9H_{17}NO_4$) C, H, N.

(3*S*,4*S*)-1-BOC-3,4-diaminopyrrolidine (3). An amount of 2.64 g (13.04 mmol) of diol **2b** was suspended in 75 mL of CH_2Cl_2. Then a totalof 2.85 mL (35.20 mmol) of dry pyridine was added and the mixture was cooled to −80 °C. An amount of 5 mL of Tf_2O was slowly added and the reaction mixture was allowed to warm to −10 °C within 2 h. The CH_2Cl_2 was carefully removed by evaporation at room temperature (heating can lead to decomposition of the labile triflate). Then 23.65 g (364 mmol) of vaccuum-dried NaN_3 and 50 mL of dry DMPU were added to the residual solid. After the suspension was stirred at room temperature for 3.5 h, a total of 100 mL of H_2O was added. The solution was extracted with MTBE (5 × 50 mL), and the combined organic extracts were washed with H_2O (3 × 50 mL) and brine (50 mL), dried over $MgSO_4$, and filtered. To avoid isolation of the explosive diazide, a total of 6 g silica gel was added and the solvent was carefully removed at room temperature. The diazide was purified by flash chromatography (hexane/EtOAc, 5:1). The azide containing fractions were combined, a total of 250 mg Pd/C was added, and the mixture was stirred under H_2 atmosphere for 14 h. The catalyst was removed by filtration over Celite, and evaporation of the filtrate yielded the diamine **3** (2.25 g, 86%), which was used without further purification. Colorless oil; ^{1}H NMR ($CDCl_3$) δ 3.77–3.46 (m, 2H), 3.10–2.96 (m, 4H), 1.57 (sbr, 4H), 1.46 (s, 9H); ^{13}C NMR ($CDCl_3$) δ 154.4, 79.3, 58.6, 58.1, 52.5, 52.1, 28.4; MS (ESI) m/z 202 (18, M + H), 224 (68, M + Na), 403 (84, 2M + H), 425 (100, 2M + Na), 604 (37, 3M + H), 626 (89, 3M + Na); HRMS (ESI) m/z calcd for $C_9H_{20}N_3O_2$ 202.155 552, found 202.156 485. Anal. ($C_9H_{19}N_3O_2$) C, H. N: calcd, 20.88; found, 20.19.

(3*S*,4*S*)-1-BOC-3,4-bis-benzenesulfonylaminopyrrolidine (4a). Following general procedure A, utilization of 183 mg (0.89 mmol) of diamine **3**, 256 μL (2.0 mmol) of benzenesulfonyl chloride, and 340 μL (2.44 mmol) of triethylamine in 5 mL of CH_2Cl_2 (22 h) yielded sulfonamide **4a** (368 mg, 86%). Colorless needles; mp 111 °C; ^{1}H NMR (DMSO-d_6) δ 8.07 (d, 2H, J = 6.9), 7.64 (t, 4H, J = 7.0), 7.66 (tt, 2H, J = 7.5, 1.5), 7.59 (t, 4H, J = 7.7), 3.52 (mul, 2H), 3.18 (dd, 2H, J = 11.5, 5.6), 2.91 (dd, 2H, J = 11.2, 3.9), 1.32 (s, 9H); ^{13}C NMR (DMSO-d_6) δ 153.0, 140.7, 132.5, 129.2, 126.4, 78.6, 56.6, 55.8, 48.6, 48.2, 28.0; MS (ESI) m/z 504 (92, M + Na), 985 (100, 2M + Na). Anal. ($C_{21}H_{27}N_3O_6S_2$) C, H, N.

(3*S*,4*S*)-1-BOC-3,4-bis-(2-chlorobenzenesulfonylamino)pyrrolidine (4c). Following general procedure A, utilization of 418 mg (2.08 mmol) of diamine **3**, 623 μL (4.57 mmol) of 2-chlorobenzenesulfonyl chloride, and 659 μL (4.98 mmol) of triethylamine in 10 mL of CH_2Cl_2 (60 h) gave rise to sulfonamide **4c** (1075 mg, 94%). Colorless needles; mp 115 °C; ^{1}H NMR ($CDCl_3$) δ 8.10 (dbr, 1H, J = 7.6), 8.04 (dbr, 1H, J = 7.6), 7.59–7.49 (m, 4H), 7.48–7.41 (m, 2H), 5.92 (sbr, 1H), 5.76 (sbr, 1H), 3.65–3.52 (m, 3H), 3.50–3.41 (m, 1H), 3.14–3.06 (m, 2H), 1.36 (s, 9H); ^{13}C NMR ($CDCl_3$) δ 153.9, 136.7, 134.4, 134.3, 131.9, 131.7, 131.5, 127.5, 80.5, 57.3, 56.3, 49.4, 48.1, 28.4; MS (ESI) m/z 572, 574, 578 (56, 46, 11, M + Na), 1121, 1123, 1125 (63, 100, 67, 2 M + Na). Anal. ($C_{21}H_{25}Cl_2N_3O_6S_2$) C, H, N.

(3*S*,4*S*)-1-BOC-3,4-bis(4-nitrobenzenesulfonylamino)pyrrolidine (4d). According to general procedure A, utilization of 425 mg (2.10 mmol) of diamine **3**, 1.024 g (4.62 mmol) of 4-nitrobenzenesulfonyl chloride, and 879 μL (6.30 mmol) of triethylamine in 20 mL of CH_2Cl_2 (22 h) yielded sulfonamide **4d** (833 mg, 69%). Colorless needles; mp 133 °C; ^{1}H NMR (MeOH-d_4) δ 8.40 (d, 2H, J = 8.5), 8.39 (d, 2H, J = 8.5), 8.10 (d, 2H, J = 8.9), 8.06 (d, 2H, J = 8.9), 3.72 (sm, 2H), 3.44 (dd, 1H, J = 11.5, 6.4), 3.37 (dd, 1H, J = 11.5, 6.4), 2.98 (dd, 1H, J = 11.5, 5.3), 2.91 (dd, 1H, J = 11.3, 5.3), 1.32 (s, 9H); ^{13}C NMR (DMSO-d_6) δ 152.9, 149.6, 146.4, 128.1, 128.0, 124.5, 78.8, 56.7, 55.9, 48.4, 48.0, 27.9; MS (ESI) m/z 594 (97, M + Na), 1165 (100, 2M + Na), 1736 (72, 3M + Na). Anal. ($C_{21}H_{25}N_5O_{10}S_2$) H, N. C: calcd, 44.13; found, 43.72.

(3*S*,4*S*)-1-BOC-3,4-bis(4-cyanobenzenesulfonylamino)pyrrolidine (4e). Following general procedure A, employment of 402 mg (2.00 mmol) of diamine **3**, 887 mg (4.40 mmol) of 4-cyanobenzenesulfonyl chloride, and 641 μL (4.40 mmol) of diisoproylethylamine in 12 mL of CH_2Cl_2 (12 h) furnished sulfonamide **4e** (759 mg, 71%). Colorless needles; mp 139 °C; ^{1}H NMR (DMSO-d_6) δ 8.39 (sbr, 2H), 8.08 (d, 4H, J = 8.3), 7.96–7.91 (m, 4H), 3.60 (sm, 2H), 3.28–3.18 (m, 2H), 2.96–2.86 (m, 2H) 1.34 (s, 9H); ^{13}C NMR (DMSO-d_6) δ 152.9, 144.8, 133.3, 127.2, 127.1, 117.6, 115.1, 78.8, 56.6, 55.9, 48.4, 47.9, 27.9; MS (ESI) m/z 554 (100, M + Na), 1085 (13, 2M + Na). Anal. ($C_{23}H_{25}N_5O_6S_2$) C, H, N.

(3*S*,4*S*)-1-BOC-3,4-bis(benzenesulfonylbenzylamino)-pyrrolidine (5ad). According to general procedure B, employment of 150 mg (0.31 mmol) of sulfonamide **4a**, 89 μL (0.75 mmol) of benzyl bromide, and 129 mg (0.93 mmol) K_2CO_3 in 2.5 mL of CH_3CN (7 h reflux) yielded, after purification by flash chromatography (hexane/MTBE, 1:1), the N-alkylated sulfonamide **5ad** (156 mg, 75%). Colorless crystals; mp 76 °C; ^{1}H NMR ($CDCl_3$) δ 7.92 (sbr, 2H), 7.73 (sbr, 4H), 7.67–7.45 (mbr, 6H), 7.34–7.02 (mbr, 10H), 4.79 (sbr, 1H), 4.45 (d, 2H, J = 15.4), 4.30 (sbr, 1H), 4.00–3.89 (m, 1H), 3.81–3.72 (m, 1H), 3.29–3.17 (mbr, 1H), 3.11–3.01 (mbr, 1H), 1.37 (s, 9H); ^{13}C NMR ($CDCl_3$) δ 153.6, 140.0, 136.4, 133.1, 129.4, 128.8, 128.2, 128.1, 127.7, 127.3, 80.2, 61.8, 60.2, 50.0, 48.9, 47.6, 46.1, 28.4; MS (ESI) m/z 684 (100, M + Na), 1345 (85, 2M + Na). Anal. ($C_{35}H_{39}N_3O_6S_2$) C, H, N.

(3*S*,4*S*)-1-BOC-3,4-bis[benzenesulfonyl-(4-iodobenzyl)amino]pyrrolidine (5af). Following general procedure B, employment of 482 mg (1.00 mmol) of sulfonamide **4a**, 713 mg (2.40 mmol) of 4-iodobenzyl bromide, and 415 mg (3.00 mmol) of K_2CO_3 in 7.5 mL of CH_3CN (7 h reflux) furnished, after purification by flash chromatography (hexane/MTBE, 2:1), the N-alkylated sulfonamide **5af** (690 mg, 76%). Light-yellow crystals; mp 98 °C; ^{1}H NMR ($CDCl_3$) δ 7.92–7.43 (mbr, 14H), 6.98–6.74 (mbr, 4H), 4.69 (sbr, 1H), 4.38 (d, 2H, J = 16.0), 4.20 (sbr, 1H), 4.02–3.90 (mbr, 1H), 3.78–3.66 (mbr, 1H), 3.33–3.09 (mbr, 2H), 3.05–2.95 (mbr, 2H), 1.39 (s, 9H); ^{13}C NMR ($CDCl_3$) δ 153.5, 139.6, 137.9, 136.0, 133.3, 130.0, 129.6, 127.6, 127.2, 93.8, 80.6, 61.9, 60.5, 49.4, 48.4, 47.5, 46.2, 28.5; MS (ESI) m/z 935 (100, M + Na), 1848 (70, 2M + Na). Anal. ($C_{35}H_{37}I_2N_3O_6S_2$) C, H, N.

(3*S*,4*S*)-1-BOC-3,4-bis[benzyl-(2-chlorobenzenesulfonyl)amino]pyrrolidine (5cd). Following general procedure B, utilization of 550 mg (1.00 mmol) of sulfonamide **4c**, 285 μL (2.40 mmol) of benzyl bromide, and 415 mg (3.00 mmol) K_2CO_3 in 7.5 mL of CH_3CN (7 h reflux) furnished, after purification by flash chromatography (hexane/EtOAc, 2:1), the N-alkylated sulfonamide **5cd** (477 mg, 65%). Beige crystals; mp 86 °C; ^{1}H NMR ($CDCl_3$) δ 7.81 (sbr, 1H), 7.65 (sbr, 1H), 7.54–7.29 (m, 4H), 7.25–6.97 (m, 12H), 4.94 (sbr, 1H), 4.70–4.51 (mbr, 3H), 4.48–4.37 (mbr, 1H), 4.26–4.17 (mbr, 1H), 3.71–3.59 (mbr, 1H), 3.46–3.35 (mbr, 1H), 3.28–3.17 (mbr, 1H), 3.13–3.03 (mbr, 1H), 1.40 (s, 9H); ^{13}C NMR ($CDCl_3$) δ 153.7, 138.3, 136.3, 135.6, 133.5, 132.1, 131.9, 131.8, 131.3, 128.5, 128.2, 127.8, 127.0, 80.3, 60.0, 58.9, 49.2, 48.4, 47.7, 47.1, 28.5; MS (ESI): m/z 752, 754, 757 (100, 87, 27 M + Na), 1481, 1483, 1485 (24, 41, 28 2M + Na). Anal. ($C_{35}H_{37}Cl_2N_3O_6S_2$) C, H, N.

(3*S*,4*S*)-1-BOC-3,4-bis[benzyl-(4-nitrobenzenesulfonyl)amino]pyrrolidine (5dd). Following the general procedure B, usage of 750 mg (1.31 mmol) of sulfonamide **4d**, 343 μl (2.89 mmol) of benzyl bromide, and 544 mg (3.94 mmol) of K_2CO_3, and a catalytic amount of KI in 10 mL of CH_3CN (4 h reflux) gave, after purification by flash chromatography (hexane/EtOAc, 2:1), the N-alkylated sulfonamide **5dd** (944 mg, 96%). Yellow crystals; mp 158 °C; ^{1}H NMR ($CDCl_3$) δ 8.31 (sbr, 4H), 7.96 (sbr, 2H), 7.83 (sbr, 2H), 7.34–7.19 (mbr, 6H), 7.12 (sbr, 4H), 4.85 (sbr, 1H), 4.45 (sbr, 3H), 4.01 (dbr, 1H, J = 13.3), 3.89 (dbr, 1H, J = 14.0), 3.36 (sbr, 1H), 3.19 (sbr, 1H), 3.09 (sbr, 2H), 1.38 (s, 9H); ^{13}C NMR ($CDCl_3$) δ 153.4, 150.1, 145.7, 135.2, 128.9, 128.6, 128.5, 128.4, 124.5, 80.7, 61.5, 60.0, 49.9, 48.0, 47.2, 46.0, 28.3; MS (ESI) m/z 774 (66, M + Na), 1525 (100, 2M + Na). Anal. ($C_{35}H_{37}N_5O_{10}S_2$) C, H, N.

(3*S*,4*S*)-1-BOC-3,4-bis[benzyl-(4-cyanobenzenesulfonyl)amino]pyrrolidine (5ed). According to general procedure B, utilization of 2.53 g (4.75 mmol) of sulfonamide **4e**, 1.35 mL (11.40 mmol) of benzyl bromide, 1.97 g (14.25 mmol) of K_2CO_3, and a catalytic amount of KI in 35 mL of CH_3CN (4 h reflux) yielded, after purification by flash chromatography (hexane/EtOAc, 2:1), the N-alkylated sulfonamide **5ed** (2.26 g, 67%). Colorless crystals; mp 208 °C; ^{1}H NMR ($CDCl_3$) δ 7.92 (sbr, 2H), 7.85–7.69 (mbr, 6H), 7.34–7.18 (mbr, 6H), 7.17–7.02 (mbr, 4H), 4.83 (sbr, 1H), 4.41 (sbr, 3H), 4.05–3.92 (mbr, 1H), 3.89–3.77 (mbr, 1H), 3.35 (sbr, 1H), 3.16–2.96 (mbr, 3H), 1.39 (s, 9H); ^{13}C NMR ($CDCl_3$) δ 153.5, 144.2, 135.3, 133.1, 129.0, 128.5, 128.4, 128.2, 127.9, 117.3, 116.8, 80.8, 61.5, 59.9, 50.0, 49.1, 47.2, 46.0, 28.4; MS (ESI) *m*/*z* 734 (67, M + Na), 1445 (100, 2M + Na). Anal. ($C_{37}H_{37}N_5O_6S_2$) C, H, N.

(3*S*,4*S*)-1-BOC-3,4-bis[(4-cyanobenzenesulfonyl)-(4-trifluoromethylbenzyl)amino]pyrrolidine (5eg). According to general procedure B, usage of 448 mg (0.84 mmol) of sulfonamide **4e**, 483 mg (2.02 mmol) of 4-trifluoromethylbenzyl bromide, and 348 mg (2.52 mmol) K_2CO_3 in 10 mL of CH_3CN (7 h, reflux) furnished, after purification by flash chromatography (hexane/EtOAc, 3:1), the N-alkylated sulfonamide **5eg** (324 mg, 45%). Colorless crystals; mp 117 °C; ^{1}H NMR ($CDCl_3$) δ 8.02–7.65 (mbr, 8H), 7.50 (sbr, 4H), 7.23 (sbr, 4H), 4.91–4.60 (mbr, 1H), 4.46 (dbr, 2H, J = 16.0), 4.32 (sbr, 1H) 4.22–3.89 (mbr, 2H), 3.59–3.21 (mbr, 2H), 3.13 (sbr, 2H), 1.41 (s, 9H); ^{13}C NMR ($CDCl_3$) δ 153.5, 143.7, 139.3, 133.3, 130.9 (q, J = 33.6), 128.6, 128.0, 125.9, 123.9 (q, J = 272.3), 117.2, 117.0, 81.3, 62.0, 60.7, 49.7, 48.5, 47.1, 46.3, 28.4; MS (ESI) *m*/*z* 870 (72, M + Na), 1717 (100, 2M + Na). Anal. ($C_{39}H_{35}F_6N_5O_6S_2$) C, H, N.

(3*S*,4*S*)-1-BOC-3,4-bis[benzyl-(4-carbamoylbenzenesulfonyl)-amino]pyrrolidine (5fd). Following general procedure C, employment of 250 mg (0.35 mmol) of nitrile **5ed**, 1.6 mL of 30% H_2O_2, and 233 mg (1.69 mmol) of K_2CO_3 in 3.2 mL of DMSO gave rise to the amide **5fd** (241 mg, 92%). Colorless crystals; mp 124 °C; ^{1}H NMR (MeOH-d_4) δ 8.08–7.95 (mbr, 4H), 7.87–7.73 (mbr, 4H), 7.34–7.13 (mbr, 10H), 4.64 (sbr, 1H), 4.59–4.49 (mbr, 3H), 3.94–3.86 (mbr, 1H), 3.82–3.74 (mbr, 1H), 3.18–3.06 (mbr, 1H), 3.03–2.81 (mbr, 3H), 1.33 (s, 9H); ^{13}C NMR (MeOH-d_4) δ 170.3, 155.0, 144.0, 139.2, 137.9, 129.8, 129.4, 129.0, 128.5, 81.6, 62.1, 61.0, 50.1, 49.9, 47.9, 47.1, 28.5; MS (ESI) *m*/*z* 770 (100, M + Na), 1517 (40, 2M + Na). Anal. ($C_{37}H_{41}N_5O_8S_2 \cdot 0.5H_2O$) C, H, N.

(3*S*,4*S*)-1-BOC-3,4-bis[(4-carbamoylbenzenesulfonyl)-(4-trifluoromethylbenzyl)amino]pyrrolidine (5fg). Following general procedure C, employment of 253 mg (0.30 mmol) of nitrile **5eg**, 1.5 mL of 30% H_2O_2, and 200 mg (1.50 mmol) of K_2CO_3 in 3.0 mL of DMSO gave rise to amide **5fg** (190 mg, 71%). Colorless crystals; mp 157 °C; ^{1}H NMR (MeOH-d_4) δ 8.04–7.92 (m, 4H), 7.89–7.72 (m, 4H), 7.53 (sbr, 4H), 7.46–7.29 (sbr, 4H), 4.78–4.53 (mbr, 4H), 4.31–4.01 (m, 2H), 3.37–3.12 (mbr, 2H), 2.97 (sbr, 2H), 1.34 (s, 9H); ^{13}C NMR (MeOH-d_4) δ 170.2, 155.5, 143.9, 142.6, 139.5, 131.0 (q, J = 31.7), 129.9, 129.8, 128.6, 126.5, 125.5 (q, J = 271.6), 81.8, 61.8, 61.0, 49.6, 48.5, 47.6, 47.0, 28.5; MS (ESI) *m*/*z* 906 (99, M + Na). Anal. ($C_{39}H_{39}F_6N_5O_8S_2$) C, H, N.

(3*S*,4*S*)-3,4-Bis[benzenesulfonylbenzylamino]pyrrolidine Hydrochloride (6ad). According to general procedure D, utilization of 102 mg (0.15 mmol) of BOC-protected pyrrolidine **5ad** and 3 mL of 2 M HCl in Et_2O gave rise to hydrochloride **6ad** (87 mg, 92%). Colorless crystals; mp 221 °C (dec); ^{1}H NMR (DMSO-d_6) δ 9.65 (sbr, 2H), 7.80 (dd, 4H, J = 8.4, 1.2), 7.72 (tt, 2H, J = 7.4, 1.2), 7.60 (tt, 4H, J = 7.8, 1.6), 7.29–7.20 (mbr, 10H), 4.80 (sm, 2H), 4.39 (d, 2H, J = 16.5), 3.97 (d, 2H, J = 16.5), 3.01 (dd, 2H, J = 11.3, 7.9), 2.78 (dd, 2H, J = 11.6, 8.1); ^{13}C NMR (DMSO-d_6) δ 139.1, 136.6, 133.3, 129.4, 128.2, 128.0, 127.4, 127.2, 57.7, 48.1, 43.2; MS (ESI) *m*/*z* 562 (100, M + H), 1123 (9, 2M + H). Anal. ($C_{30}H_{31}N_3O_4S_2 \cdot HCl \cdot 0.5H_2O$) H, N. C: calcd, 59.34; found, 59.75.

(3*S*,4*S*)-3,4-Bis[benzenesulfonyl-(4-iodobenzyl)amino]pyrrolidine Hydrochloride (6af). Following the general procedure D, usage of 183 mg (0.20 mmol) of BOC-protected pyrrolidine **5af** and 5 mL of 2 M HCl in Et_2O yielded hydrochloride **6af** (138 mg, 81%). Beige crystals; mp 211 °C (dec); ^{1}H NMR (MeOH-d_4) δ 7.87 (dd, 4H, J = 7.1, 1.1), 7.74 (t, 2H, J = 7.4), 7.63 (t, 4H, J = 7.7), 7.63 (t, 4H, J = 8.3), 6.89 (d, 4H, J = 8.3), 4.68 (sm, 2H), 4.34 (d, 2H, J = 16.0), 3.92 (d, 2H, J = 16.3), 3.46–3.38 (m, 2H), 3.34–3.24 (m, 2H); ^{13}C NMR (MeOH-d_4) δ 140.5, 139.2, 136.9, 135.0, 131.4, 130.9, 128.8, 94.6, 62.2, 51.1, 47.5; MS (ESI) *m*/*z* 814 (100, M + H). Anal. ($C_{30}H_{29}I_2N_3O_4S_2 \cdot HCl$) C, H, N.

(3*S*,4*S*)-3,4-Bis[benzyl-(2-chlorobenzenesulfonyl)amino]pyrrolidine Hydrochloride (6cd). Following general procedure D, employment of 138 mg (0.20 mmol) of BOC-protected pyrrolidine **5cd** and 5 mL of 2 M HCl in Et_2O yielded hydrochloride **6cd** (104 mg, 78%). Beige crystals; mp 172 °C (dec); ^{1}H NMR ($CDCl_3$) δ 9.87 (sbr, 2H), 7.73 (d, 2H, J = 7.8), 7.43 (dd, 2H, J = 7.3, 0.9), 7.38 (td, 2H, J = 7.6, 1.1), 7.13 (t, 2H, J = 7.3), 7.10–7.04 (mbr, 10H), 4.97 (sm, 2H), 4.59 (d, 2H, J = 15.8), 4.37 (d, 2H, J = 15.8), 3.49 (sbr, 2H), 3.12 (sbr, 2H); ^{13}C NMR ($CDCl_3$) δ 137.9, 135.3, 133.8, 132.2, 131.9, 131.6, 128.8, 128.5, 128.1, 127.2, 58.4, 49.1, 45.6; MS (ESI) *m*/*z* 630, 632, 634 (100, 90, 25, M + H). Anal. ($C_{30}H_{29}Cl_2N_3O_4S_2 \cdot HCl \cdot H_2O$) C, H, N.

(3*S*,4*S*)-3,4-Bis[benzyl-(4-carbamoylbenzenesulfonyl)amino]-pyrrolidine Hydrochloride (6fd). Following general procedure D, usage of 135 mg (0.18 mmol) of BOC-protected pyrrolidine **5fd** and 5 mL of 2 M HCl in Et_2O gave rise to hydrochloride **6fd** (100 mg, 81%). Colorless crystals; mp 176 °C (dec); ^{1}H NMR (DMSO-d_6) δ 8.21 (sbr, 1H), 8.02 (d, 4H, J = 8.5), 7.75 (d, 4H, J = 8.5), 7.62 (sbr, 1H), 7.35–7.24 (mbr, 10H), 4.47 (d, 2H, J = 16.3), 4.33 (sbr, 2H), 4.17 (d, 2H, J = 16.3), 2.59–2.51 (m, 2H), 2.25 (dd, 2H, J = 10.6, 4.7); ^{13}C NMR (DMSO-d_6) δ 166.3, 141.5, 137.9, 137.5, 128.3, 128.1, 127.8, 127.2, 126.9, 61.7, 48.2, 47.6; MS (ESI) *m*/*z* 648 (100, M + H), 1295 (10, 2M + H). Anal. ($C_{32}H_{33}N_5O_6S_2 \cdot HCl \cdot 0.5H_2O$) C, H, N.

(3*S*,4*S*)-3,4-Bis[benzyl-(4-aminobenzenesulfonyl)amino]pyrrolidine Trihydrochloride (6gd). A total of 608 mg (0.81 mmol) of nitrosulfonamide **5dd** was dissolved in 30 mL of EtOAc. After addition of 1.82 g (8.1 mmol) of $SnCl_2 \cdot 2H_2O$, the suspension was heated to reflux for 2 h and subsequently allowed to reach room temperature. Following the addition of 10 mL of aqueous saturated $NaHCO_3$ solution, the aqueous phase was separated and extracted with EtOAc (3 × 10 mL). The combined organic phases were washed with brine (3 × 10 mL), dried over Na_2SO_4, filtered, and evaporated. The remaining solid was dissolved in 5 mL of dry Et_2O, and 5 mL of 2 M HCl in Et_2O was added. After 12 h at room temperature, the solution was decanted from the precipitate, which was washed with Et_2O and dried in vacuum, yielding trihydrochloride **6gd** (445 mg, 79%). Yellow crystals; mp 176 °C (dec); ^{1}H NMR (MeOH-d_4) δ 7.43 (d, 4H, J = 8.3), 7.37–7.25 (m, 6H), 7.07 (d, 4H, J = 6.6), 6.71 (d, 4H, J = 8.5), 4.59 (sbr, 2H), 4.12 (d, 2H, J = 15.4), 3.85 (d, 2H, J = 15.6), 3.48–3.36 (m, 4H); ^{13}C NMR (MeOH-d_4) δ 154.9, 134.5, 131.0, 129.9, 129.6, 129.2, 125.1, 114.7, 62.3, 51.9, 48.2; MS (ESI) *m*/*z* 592 (100, M + H), Anal. ($C_{30}H_{29}N_5O_4S_2 \cdot 3HCl \cdot 4H_2O$) C, H, N.

(3*S*,4*S*)-3,4-Bis[(4-carbamoylbenzenesulfonyl)-(4-trifluoromethylbenzyl)amino]pyrrolidine Hydrochloride (6fg). Following general procedure D, employment of 148 mg (0.17 mmol) of BOC-protected pyrrolidine **5fg** and 5 mL of 2 M HCl in Et_2O furnished hydrochloride **6fg** (110 mg, 80%). Yellow crystals; mp 194 °C (dec); ^{1}H NMR (DMSO-d_6) δ 9.79 (sbr, 2H), 8.23 (sbr, 2H), 8.04 (sbr, 4H), 7.83 (sbr, 4H), 7.64 (sbr, 8H), 7.60 (sbr, 2H), 4.90 (sbr, 2H), 4.58 (sbr, 2H), 3.07 (sbr, 2H), 2.76 (sbr, 2H); ^{13}C NMR (DMSO-d_6) δ 165.9, 141.5, 140.1, 138.1, 128.3, 128.2, 127.5 (q, J = 32.6), 127.1, 124.5, 123.9 (q, J = 273.5), 57.6, 47.1, 42.1; MS (ESI) *m*/*z* 784 (100, M + H). Anal. ($C_{34}H_{31}F_6N_5O_6S_2 \cdot HCl \cdot 4H_2O$) C, H, N.

Acknowledgment. We acknowledge the support of the beamline staff at BESSY II, Berlin, Germany, as well as the beamline staff at EMBL/DESY, Hamburg, Germany. The pET11a plasmid containing the HIV-1 protease gene was kindly provided by Professor Helena Danielson, University of Uppsala, Sweden. This work was also supported by a fellowship (A.B.)

from the Fonds der Chemischen Industrie (FCI) and by the Deutsche Pharmazeutische Gesellschaft (DPhG) "Stiftung zur Förderung des wissenschaftlichen Nachwuchses" (W.E.D.).

Supporting Information Available: Combustion analysis results, crystallographic data, and additional details of experimental procedure. This material is available free of charge via the Internet at http://pubs.acs.org.

References

(1) *UNAIDS: 2006 Report on the Global AIDS Epidemic*; UNAIDS: Geneva, 2006.

(2) Pomerantz, R. J.; Horn, D. L. Twenty years of therapy for HIV-1 infection. *Nat. Med.* **2003**, *9* (7), 867–873.

(3) Wlodawer, A.; Erickson, J. W. Structure-based inhibitors of HIV-1 protease. *Annu. Rev. Biochem.* **1993**, *62* (1), 543–585.

(4) Rodríguez-Barrios, F.; Gago, F. HIV protease inhibition: limited recent progress and advances in understanding current pitfalls. *Curr. Top. Med. Chem.* **2004**, *4*, 991–1007.

(5) Chrusciel, R. A.; Strohbach, J. W. Non-peptidic HIV protease inhibitors. *Curr. Top. Med. Chem.* **2004**, *4* (10), 1097–1114.

(6) Randolph, J. T.; DeGoey, D. A. Peptidomimetic inhibitors of HIV protease. *Curr. Top. Med. Chem.* **2004**, *4* (10), 1079–1095.

(7) D'Aquila, R. T.; Schapiro, J. M.; Brun-Vézinet, F.; Clotet, B.; Conway, B.; Demeter, L. M.; Grant, R. M.; Johnson, V. A.; Kuritzkes, D. R.; Loveday, C.; Shafer, R. W.; Richman, D. D. Drug resistance mutations in HIV-1. *Top. HIV Med.* **2002**, *10* (5), 21–25.

(8) Güller, R.; Binggeli, A.; Breu, V.; Bur, D.; Fischli, W.; Hirth, G.; Jenny, C.; Kansy, M.; Montavon, F.; Müller, M.; Oefner, C.; Stadler, H.; Vieira, E.; Wilhelm, M.; Wostl, W.; Märki, H. P. Piperidine−renin inhibitors compounds with improved physicochemical properties. *Bioorg. Med. Chem. Lett.* **1999**, *9* (10), 1403–1408.

(9) Vieira, E.; Binggeli, A.; Breu, V.; Bur, D.; Fischli, W.; Güller, R.; Hirth, G.; Märki, H. P.; Müller, M.; Oefner, C.; Scalone, M.; Stadler, H.; Wilhelm, M.; Wostl, W. Substituted piperidines−highly potent renin inhibitors due to induced fit adaptation of the active site. *Bioorg. Med. Chem. Lett.* **1999**, *9* (10), 1397–1402.

(10) John, V.; Beck, J. P.; Bienkowski, M. J.; Sinha, S.; Heinrikson, R. L. Human β-secretase (BACE) and BACE inhibitors. *J. Med. Chem.* **2003**, *46* (22), 4625–4630.

(11) Prade, L.; Jones, A. F.; Boss, C.; Richard-Bildstein, S.; Meyer, S.; Binkert, C.; Bur, D. X-ray structure of plasmepsin II complexed with a potent achiral inhibitor. *J. Biol. Chem.* **2005**, *280* (25), 23837–23843.

(12) Hof, F.; Schütz, A.; Fäh, C.; Meyer, S.; Bur, D.; Liu, J.; Goldberg, D. E.; Diederich, F. Starving the malaria parasite: inhibitors active against the aspartic proteases plasmepsins I, II, and IV. *Angew. Chem., Int. Ed.* **2006**, *45* (13), 2138–2141.

(13) Specker, E.; Böttcher, J.; Lilie, H.; Heine, A.; Schoop, A.; Müller, G.; Griebenow, N.; Klebe, G. An old target revisited: two new privileged skeletons and an unexpected binding mode for HIV-protease inhibitors. *Angew. Chem., Int. Ed.* **2005**, *44* (20), 3140–3144.

(14) Specker, E.; Böttcher, J.; Brass, S.; Heine, A.; Lilie, H.; Schoop, A.; Müller, G.; Griebenow, N.; Klebe, G. Unexpected novel binding mode of pyrrolidine-based aspartyl protease inhibitors: design, synthesis and crystal structure in complex with HIV protease. *ChemMedChem* **2006**, *1* (1), 106–117.

(15) Czodrowski, P.; Sotriffer, C. A.; Klebe, G. Atypical protonation states in the active site of HIV-1 protease: a computational study. *J. Chem. Inf. Model.* **2007**, *47* (4), 1590–1598.

(16) Nagel, U. Asymmetric hydrogenation of α-(acetylamino)cinnamic acid with a novel rhodium complex; the design of an optimal ligand. *Angew. Chem., Int. Ed. Engl.* **1984**, *23* (6), 435–436.

(17) Nagel, U.; Kinzel, E.; Andrade, J.; Prescher, G. Enantioselektive Katalyse, 4. Synthese *N*-substituierter (*R*,*R*)-3,4-Bis(diphenylphosphino)-pyrrolidine und Anwendung ihrer Rhodiumkomplexe zur asymmetrischen Hydrierung von α-(Acylamino)-acrylsäure-Derivaten. Enantioselective Catalysis, 4. Synthesis *N*-Substituted (*R*,*R*)-3,4-Bis(diphenylphosphino)-pyrrolidines. The Use of their Rhodium Complexes for the Asymmetric Hydrogenation of α-(Acylamino)-acrylic Acid Derivatives. *Chem. Ber.* **1986**, *119* (11), 3326–3343.

(18) Rocha Gonsalves, A. M. d. A.; Serra, M. E. S.; Murtinho, D.; Silva, V. F.; Matos Beja, A.; Paixão, J. A.; Ramos Silva, M.; Alte da Veiga, L. Pyrrolidine-based amino alcohols: novel ligands for the enantioselective alkylation of benzaldehyde. *J. Mol. Catal. A: Chem.* **2003**, *195* (1–2), 1–9.

(19) Skarøewski, J.; Gupta, A. Synthesis of C_2 symmetric primary vicinal diamines. Double stereospecific Mitsunobu reaction on the heterocyclic diols derived from tartaric acid. *Tetrahedron: Asymmetry* **1997**, *8* (11), 1861–1867.

(20) Rodríguez Sarmiento, R. M.; Wirz, B.; Iding, H. Chemoenzymatic preparation of non-racemic *N*-Boc-pyrrolidine-3,4-dicarboxylic acid 3-ethyl esters and their 4-hydroxymethyl derivatives. *Tetrahedron: Asymmetry* **2003**, *14* (11), 1547–1551.

(21) Kuppert, D.; Sander, J.; Roth, C.; Wörle, M.; Weyhermüller, T.; Reiss, G. J.; Schilde, U.; Müller, I.; Hegetschweiler, K. The coordination chemistry of *cis*-3,4-diaminopyrrolidine and related polyamines. *Eur. J. Inorg. Chem.* **2001**, (10), 2525–2542.

(22) Song, C. E.; Yang, J. W.; Roh, E. J.; Lee, S.-G.; Ahn, J. H.; Han, H. Heterogeneous Pd-catalyzed asymmetric allylic substitution using resin-supported trost-type bisphosphane ligands. *Angew. Chem., Int. Ed.* **2002**, *41* (20), 3852–3854.

(23) Katritzky, A. R.; Pilarski, B.; Urogdi, L. Efficient conversion of nitriles to amides with basic hydrogen peroxide in dimethyl sulfoxide. *Synthesis* **1989**, (12), 949–950.

(24) Kettler, K.; Sakowski, J.; Wiesner, J.; Ortmann, R.; Jomaa, H.; Schlitzer, M. Novel lead structures for antimalarial farnesyltransferase inhibitors. *Pharmazie* **2005**, *60* (5), 323–327.

(25) Taylor, A.; Brown, D. P.; Kadam, S.; Maus, M.; Kohlbrenner, W. E.; Weigl, D.; Turon, M. C.; Katz, L. High-level expression and purification of mature HIV-1 protease in *Escherichia coli* under control of the *araBAD* promoter. *Appl. Microbiol. Biotechnol.* **1992**, *37* (2), 205–210.

(26) Toth, M. V.; Marshall, G. R. A simple, continuous fluorometric assay for HIV protease. *Int. J. Pept. Protein Res.* **1990**, *36* (6), 544–550.

(27) Otwinowski, Z.; Minor, W. Processing of X-ray Diffraction Data Collected in Oscillation Mode. In *Methods in Enzymology*; Carter, C. W., Jr., Ed.; Academic Press: San Diego, CA, 1997; Vol. 276, pp 307–326.

(28) Storoni, L. C.; McCoy, A. J.; Read, R. J. Likelihood-enhanced fast rotation functions. *Acta Crystallogr. D* **2004**, *60* (3), 432–438.

(29) Pape, T.; Schneider, T. R. HKL2MAP: a graphical user interface for macromolecular phasing with SHELX programs. *J. Appl. Crystallogr.* **2004**, *37* (5), 843–844.

(30) Usón, I.; Sheldrick, G. M. Advances in direct methods for protein crystallography. *Curr. Opin. Struct. Biol.* **1999**, *9* (5), 643–648.

(31) Sheldrick, G. M. Macromolecular phasing with SHELXE. *Z. Kristallogr.* **2002**, *217* (12), 644–650.

(32) Cowtan, K. D.; Zhang, K. Y. J. Density modification for macromolecular phase improvement. *Prog. Biophys. Mol. Biol.* **1999**, *72* (3), 245–270.

(33) Lamzin, V. S.; Wilson, K. S. Automated refinement of protein models. *Acta Crystallogr. D* **1993**, *49* (1), 129–147.

(34) The CCP4 suite: programs for protein crystallography. *Acta Crystallogr. D* **1994**, *50* (5), 760–763.

(35) Brünger, A. T.; Adams, P. D.; Clore, G. M.; DeLano, W. L.; Gros, P.; Grosse-Kunstleve, R. W.; Jiang, J.-S.; Kuszewski, J.; Nilges, M.; Pannu, N. S.; Read, R. J.; Rice, L. M.; Simonson, T.; Warren, G. L. Crystallography & NMR system: a new software suite for macromolecular structure determination. *Acta Crystallogr. D* **1998**, *54* (5), 905–921.

(36) Sheldrick, G. M.; Schneider, T. R., SHELXL: High-Resolution Refinement. In *Methods in Enzymology*; Charles, W. C. J., Robert, M. S., Eds.; Academic Press: San Diego, CA, 1997; Vol. 277, pp 319–343.

(37) Emsley, P.; Cowtan, K. Coot: model-building tools for molecular graphics. *Acta Crystallogr. D* **2004**, *60* (12, Part 1), 2126–2132.

JM701142S